

## Research Article

# Polycrystalline Silicon Thin-Film Solar Cells on AIT-Textured Glass Superstrates

Per I. Widenborg and Armin G. Aberle

*Photovoltaics Centre of Excellence, The University of New South Wales (UNSW), Sydney, NSW 2052, Australia*

Received 29 April 2007; Revised 24 September 2007; Accepted 25 September 2007

Recommended by Xian An Cao

A new glass texturing method (AIT—aluminium-induced texturisation) has recently been developed by our group. In the present work, the potential of this method is explored by fabricating PLASMA poly-Si thin-film solar cells on glass superstrates that were textured with the AIT method. Using an interdigitated metallisation scheme with a full-area Al rear contact, PLASMA cells with an efficiency of up to 7% are realised. This promising result shows that the AIT glass texturing method is fully compatible with the fabrication of poly-Si thin-film solar cells on glass using solid phase crystallisation (SPC) of PECVD-deposited amorphous silicon precursor diodes. As such, there are now two distinctly different glass texturing methods—the AIT method and CSG Solar's glass bead method—that are known to be capable of producing efficient SPC poly-Si thin-film solar cells on glass.

Copyright © 2007 P. I. Widenborg and A. G. Aberle. This is an open access article distributed under the Creative Commons Attribution License, which permits unrestricted use, distribution, and reproduction in any medium, provided the original work is properly cited.

## 1. INTRODUCTION

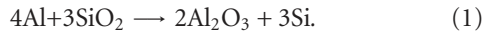
Polycrystalline silicon (poly-Si) thin-film device structures on inexpensive foreign supporting materials such as glass are becoming increasingly important, for example in thin-film solar cells and flat panel displays. In the case of solar cells, thin-films have the potential to significantly reduce the cost of manufacture of photovoltaic (PV) modules due to the fact that they only require a fraction of the silicon material as compared to traditional, silicon wafer-based modules. Furthermore, thin-film poly-Si solar cells have the advantage that it is possible to manufacture them on large-area supporting materials ( $\sim 1 \text{ m}^2$ ), streamlining the production process and further reducing processing costs. The efficiency of solar cells based on poly-Si materials (i.e., materials with a grain size larger than about  $1 \mu\text{m}$ , no amorphous tissue) is also intrinsically more stable compared to that of cells based on amorphous or microcrystalline silicon thin-films.

Due to the weak absorption of near-infrared light in crystalline silicon (c-Si), an effective light trapping scheme is essential for poly-Si thin-film solar cells (i.e., Si thickness of less than  $10 \mu\text{m}$ ). One effective way to obtain light trapping is to texture the supporting material prior to the deposition of the Si film. As a result of the texture, light is transmitted obliquely into the Si film, significantly enhancing the optical pathlength and thus increasing the optical absorption.

A texture that has steeper slopes will increase the optical absorption more strongly than a shallow texture. The optical absorption is further enhanced by depositing a high-quality reflector onto the back surface (back surface reflector—BSR). Best optical absorption is obtained if the texture and the BSR are optimised such that the total internal reflection occurs both at the front and the rear surface of the Si film, enabling multiple passes of the light through the solar cell. Apart from the light trapping benefits, the textured substrate also reduces reflection losses at the front surface of the solar cell (double-bounce effect). The most efficient poly-Si thin-film solar cells made as yet at low temperature on foreign supporting materials have energy conversion efficiencies in the range 9–10% and were fabricated by solid phase crystallization (SPC) at about  $600^\circ\text{C}$  of hydrogenated amorphous silicon (a-Si:H) precursor diodes on a textured metal substrate (9.2%) [1] or a textured glass superstrate (9.8%) [2, 3]. The a-Si:H precursor diodes were deposited by plasma-enhanced chemical vapor deposition (PECVD). Besides giving good cell efficiency, the SPC method has a number of other advantages such as simplicity of the process and low cost.

In the present work, we use the SPC method to fabricate poly-Si thin-film solar cells on glass superstrates that are textured with a new method recently developed by us [4, 5]. This method is referred to as aluminium-induced texturisation (AIT) and is based on a thermally activated chemical reaction

between the glass and a thin, sacrificial aluminium layer. All sacrificial Al films used in the present work were deposited by evaporation. The high temperature ( $\sim 600^\circ\text{C}$ ) during the subsequent thermal anneal induces a spatially nonuniform redox reaction between the Al and the glass ( $\text{SiO}_2$ ) according to



Following this anneal, the reaction products ( $\text{Al}_2\text{O}_3$ , Si) are removed by wet chemical etching. The Al layer can be deposited by evaporation or sputtering and hence the AIT method is suitable for large-area applications such as thin-film PV. All solar cells reported in this paper are made by SPC of PECVD-deposited a-Si:H precursor diodes and are referred to by us as “PLASMA” cells [6]. In addition to AIT-textured glass sheets, we also use planar glass sheets to clearly reveal the benefits of the glass texture. The cells are analysed structurally (focused ion beam microscopy, atomic force microscopy), optically (reflectance, transmission), and electrically (1-Sun current-voltage, external and internal quantum efficiency). Computer simulations are also performed to determine the cells’ light trapping properties and the diffusion length in the absorber region.

## 2. EXPERIMENTAL DETAILS

A resistively heated evaporator (Varian) was used for depositing aluminium onto clean  $15 \times 15 \text{ cm}^2$  glass sheets from Schott AG (Borofloat33, 3.3 mm thick). The thickness of the evaporated Al films was in the range of 40 to 230 nm. The evaporation rate was in the range of 3 nm/sec. The samples were then annealed at  $610^\circ\text{C}$  for 40 minutes in a nitrogen purged tube furnace, inducing a chemical reaction between the glass substrate and the aluminium layer. Removal of the aluminium layer and the reaction products was realised by immersion for 10 minutes in hot ( $130^\circ\text{C}$ ) concentrated (85%) phosphoric acid, followed by a 10-second dip in a 1:1 HF:HNO<sub>3</sub> solution. A conventional 13.56-MHz parallel-plate PECVD system (MV Systems, USA) was used for depositing a SiN layer (used as a diffusion barrier and antireflection coating with a thickness of  $\sim 70 \text{ nm}$  and a refractive index of  $\sim 2.05$ ) and a-Si:H precursor diodes onto planar and AIT textured  $15 \times 15 \text{ cm}^2$  sheets. Gas mixtures of pure silane with 0.5% phosphine in silane, 100 ppm diborane in hydrogen, and 0.5% trimethylboron in hydrogen were used for the deposition of  $n^+$ ,  $p^-$ , and  $p^+$  doped a-Si:H films, respectively. The total silane gas flow was kept fixed at 40 sccm, the total pressure was about 800 mTorr, the glass temperature about  $400^\circ\text{C}$ , and the RF power about  $25 \text{ mW/cm}^2$ . The SPC anneals (19 hours at about  $600^\circ\text{C}$ ) were performed ex situ in a conventional nitrogen-purged atmospheric pressure tube furnace. Following crystallisation, one  $5 \times 5 \text{ cm}^2$  sample was cut from the centre of each  $15 \times 15 \text{ cm}^2$  glass sheet. The samples then received an RTA process at  $900\text{--}1000^\circ\text{C}$  for up to 5 minutes, followed by a hydrogenation treatment. The hydrogenation was performed in a cold-wall vacuum system featuring an inductively coupled remote plasma source (Advanced Energy, USA), using a glass temperature

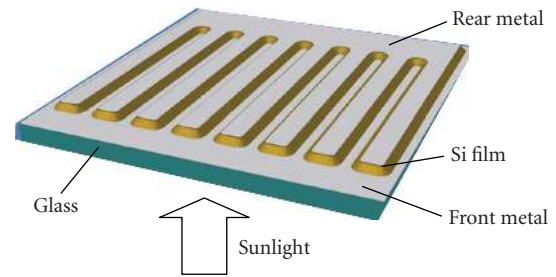


FIGURE 1: Schematic representation of the interdigitated metallisation scheme of our poly-Si thin-film solar cells on glass. The drawing illustrates a part of one cell (not to scale).

of  $610\text{--}640^\circ\text{C}$  during 15–30 minutes, a plasma power of 3200–3500 W, a hydrogen gas flow of 200 sccm, and an argon gas flow of 60 sccm [7]. The metallisation scheme used in this work consists of two interdigitated comb-like metal grids, as schematically shown in Figure 1. The rear metal grid ( $\sim 600 \text{ nm}$  thick Al) serves as the rear (i.e., air-side) electrode of the cell, the back surface reflector, and a mask for plasma etching of the grooves for the front electrode. The comb-like, front (i.e., glass-side) electrode also consists of Al and can be formed in several ways, for instance, using the self-aligned maskless photolithography (SAMPL) method [8]. The front finger spacing of the cells is 0.56 mm and the cell dimension is 1.1 cm by 4.0 cm. Each  $5 \times 5 \text{ cm}^2$  glass piece features four PLASMA solar cells of dimension 1.1 cm by 4.0 cm.

The fabricated PLASMA solar cells were investigated by optical reflectance and transmission spectroscopy (Varian Cary 5G, double-beam spectrophotometer with an integrating sphere) and the surface morphology of the cells was investigated by Focused Ion Beam microscopy (FEI xP200) and Atomic Force Microscopy (AFM). After metallisation, the solar cells were characterised by current-voltage ( $I$ - $V$ ) and external and internal quantum efficiency (EQE, IQE) measurements. The optical spectroscopy measurements as well as the EQE measurements were carried out in the superstrate configuration, using perpendicular illumination of the samples. The solar cell simulation program PC1D [9] was used to estimate the absorber region diffusion lengths and the light trapping properties of the PLASMA poly-Si thin-film solar cells.

## 3. RESULTS

### 3.1. Structural and optical properties

Figure 2 shows the surface morphology of a representative PLASMA solar cell grown on AIT-textured glass, revealing a cauliflower-like structure. In Figure 3, AFM measurements show how the roughness of the bare glass texture varies with the Al thickness used in the AIT process. As can be seen, maximum glass surface roughness is obtained for an Al thickness in the 160–200 nm range.

The impact of the AIT glass texture on the optical absorbance  $A(\lambda)$  of PLASMA cells with a silicon thickness of  $2 \mu\text{m}$  is shown in Figure 4. The bottom curve was measured on a planar cell, the middle curve on a cell textured with

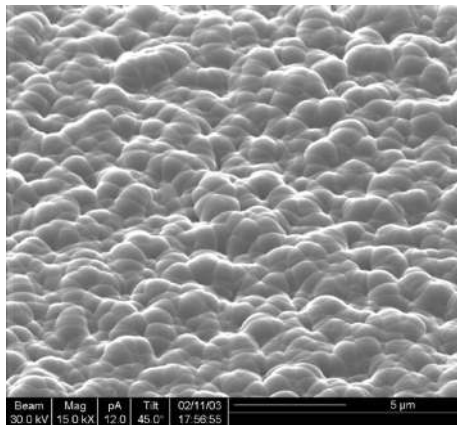


FIGURE 2: Focused ion beam (FIB) image of the rear surface of a PLASMA solar cell grown on an AIT-textured glass sheet. The length of the marker is  $5\ \mu\text{m}$ .

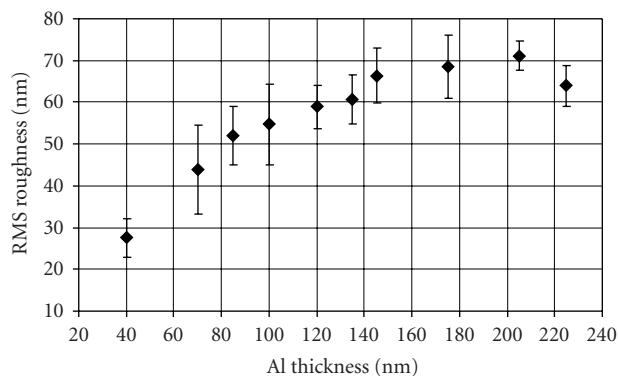


FIGURE 3: Results from AFM measurements showing how the roughness of the bare glass texture (i.e., no silicon film) varies with the Al thickness used in the AIT process.

70 nm of Al in the AIT process, and the top curve on a cell textured with 175 nm of Al in the AIT process. These absorbance results were obtained via  $A = 1 - (R + T)$ , where  $R$  and  $T$  are the measured hemispherical reflectance and transmission. These measurements were taken before the cells were metallised, and hence the back surface reflector (BSR) was air at this stage. As can be seen, compared to the planar sample, the AIT-70 nm glass almost doubles the absorbance at  $\lambda = 800\ \text{nm}$ , while the corresponding boost for the AIT-175 nm glass is even greater ( $\sim 2.5$  times). Combined with the AFM roughness results of Figure 3, these results clearly show that a rougher AIT glass surface leads to more efficient scattering and trapping of light, and hence to a larger optical absorption. For wavelengths above 800 nm, absorption in the 3 mm thick glass sheet becomes increasingly important, particularly for textured glass. As shown in [10], absorption in 3 mm thick AIT-textured glass sheets dominates over absorption in the Si thin-film for  $\lambda > 950\ \text{nm}$ , and this explains the significant absorption of the textured samples at wavelengths above the c-Si bandgap ( $\sim 1100\ \text{nm}$ ). The improved absorbance at short wavelengths ( $\lambda < 500\ \text{nm}$ ) for the top curve in Figure 4 is due to reduced front surface reflec-

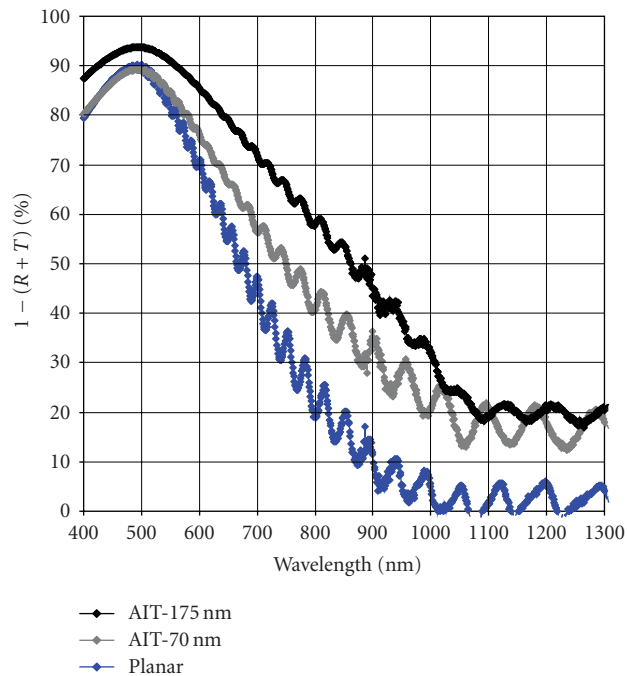


FIGURE 4: Wavelength-dependent optical absorbance  $A$  of a planar PLASMA cell (bottom curve) and two AIT-textured PLASMA cells (top curve = AIT-175 nm). Poly-Si thickness is about  $2\ \mu\text{m}$  in each case. The intended structure of the samples is glass/SiN/ $n^+p^-p^+$ .

tion caused by the rougher front surface of this Si solar cell (double-bounce effect).

The impact of the silicon film thickness on the optical absorbance  $A(\lambda)$  of planar and AIT-textured PLASMA cells is shown in Figure 5. These measurements were again taken before the cells were metallised and hence the BSR was again air. For cells on planar glass, increasing the Si thickness from 2 to  $5\ \mu\text{m}$  strongly improves the optical absorption in the 500–900 nm wavelength band (e.g., by a factor of  $\sim 1.6$  at  $\lambda = 800\ \text{nm}$ ). This is a direct consequence of the poor light trapping properties of planar cells, necessitating the use of a relatively thick planar Si film ( $>10\ \mu\text{m}$ ) to obtain good absorption of the solar spectrum. In contrast, due to good light trapping, the optical absorption of textured samples increases only slightly (e.g., by a factor of  $\sim 1.1$  at  $\lambda = 800\ \text{nm}$ ) when the Si thickness is increased from 2 to  $5\ \mu\text{m}$ . This shows that a Si thickness of  $5\ \mu\text{m}$  is more than enough for PLASMA poly-Si cells on AIT-textured glass to ensure a good absorption of the solar spectrum, provided that the back surface reflector is of high quality. It should be noted that the optical properties of the SiN antireflective coating affect the absorption curves shown in Figures 4 and 5. However, all SiN layers used in this work were nominally identical and hence the conclusions drawn from Figures 4 and 5 remain unaffected.

### 3.2. Current-voltage and quantum efficiency measurements

Upon completion of the absorption measurements, several samples were metallised and their 1-Sun  $I$ - $V$  curve measured

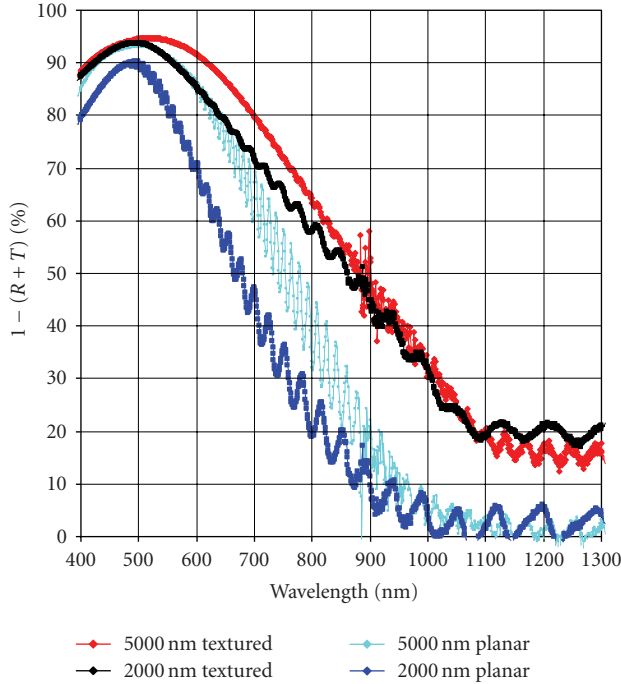


FIGURE 5: Wavelength-dependent optical absorbance  $A$  of two planar PLASMA cells (bottom curves, Si thickness 2 and  $5\ \mu\text{m}$ ) and two AIT-textured PLASMA cells (top curves, Si thickness 2 and  $5\ \mu\text{m}$ ). Both textured glass sheets were fabricated with an Al thickness of 175 nm in the AIT process. The structure of the samples is the same as in Figure 4.

on a halogen-lamp-based solar simulator. Additionally, the reflectance and the external quantum efficiency of these samples were measured. From each measured EQE curve, the 1-Sun short-circuit current ( $J_{sc,EQE}$ ) for the standard terrestrial solar spectrum (AM1.5G,  $100\ \text{mW}/\text{cm}^2$ ) was calculated. The results of the 1-Sun  $I$ - $V$  measurements are shown in Table 1, together with the corresponding  $J_{sc,EQE}$  values. Several representative EQE curves are shown in Figure 6. As can be seen from Table 1, reasonable agreement (2–9% relative difference) between the  $J_{sc}$  values obtained from the  $I$ - $V$  and EQE measurements is obtained.

Two important conclusions can be drawn from Table 1. The first is that the glass texture does not negatively affect the  $V_{oc}$  and the  $FF$  of the PLASMA cells, confirming that the AIT glass texturing method is well suited to the fabrication of these thin-film solar cells. Secondly, the  $J_{sc}$  of PLASMA cells is significantly boosted by the AIT glass texture, giving the textured cells a clear efficiency advantage (about 8–19% relative) over their planar counterparts. The highest efficiency obtained in Table 1 is 5.5%, which is a clear proof-of-concept for PLASMA solar cells on AIT-textured glass.

Taking a closer look at the short-circuit currents in Table 1, it can be seen that, for a given Si solar cell thickness, the introduction of the glass texture increases the cell's short-circuit current (EQE) by 5–17%. While this is a significant enhancement, it is well below the enhancement that might have been expected from the absorption measurements performed on the samples prior to metallisation

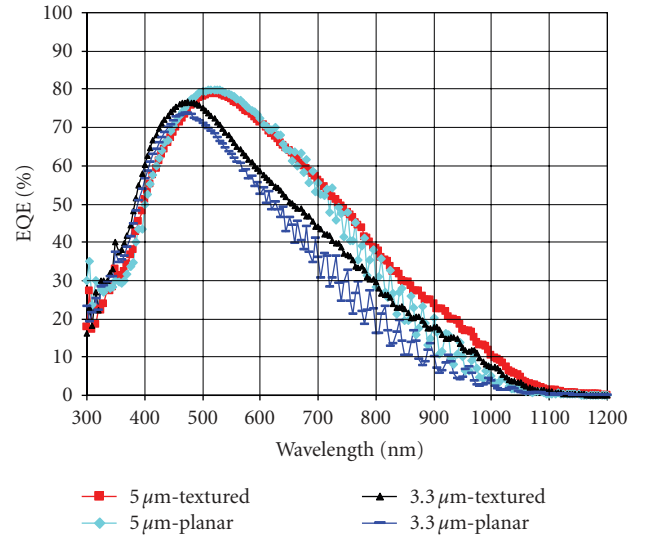


FIGURE 6: Measured EQE of two  $3.3\ \mu\text{m}$  thick PLASMA solar cells (1  $\times$  planar, 1  $\times$  textured) and two  $5.0\ \mu\text{m}$  thick PLASMA solar cells (1  $\times$  planar, 1  $\times$  textured).

(see Section 3.1). One possible reason could be a very small minority-carrier diffusion length  $L$  in the cells' absorber region (i.e.,  $L \ll W_{ab}$ , where  $W_{ab}$  is the width of the absorber layer), causing a poor  $J_{sc}$  despite good optical absorption of the solar spectrum in the Si film. To test this hypothesis, the external quantum efficiency curves of several cells were fitted with the 1-dimensional solar cell simulator PC1D [9]. Good agreement between measured and simulated EQE curves was obtained, as shown in Figure 7. The corresponding PC1D parameters are given in Table 2. To fit the short-wavelength response of these PLASMA solar cells, it was necessary to insert a lightly doped ( $1 \times 10^{16}\ \text{cm}^{-3}$ )  $n$ -type region between the highly doped  $n$ -type emitter and the lowly doped  $p$ -type part of the absorber layer, giving a  $n^+n^-p^-p^+$  solar cell structure. Sheet resistance profiling has recently shown that such a structure is typical for our present PLASMA solar cells [11]. As can be seen from Table 2, the absorber region diffusion lengths of all samples are similar to the width of the corresponding region of the absorber and hence the modest current gains due to the glass texture are *not* due to a poor diffusion length in the absorber region. Instead, modeling of the cells' EQE with PC1D reveals that the modest  $J_{sc}$  gain due to the texture is caused by a severe degradation of the internal reflection at the rear surface of the cells. Specifically, PC1D determines an internal rear reflection of about 50% at the planar Si/Al interface, whereas the corresponding value is only about 25% at the textured Si/Al interface. We believe that the poor internal reflectance of the textured samples is due to the double-bounce effect at textured rear surfaces, reducing the internal rear reflectance to  $(1/2)^2 = 0.25 = 25\%$ . These results are also in good agreement with [12] where it was found that depositing a layer of white paint (which acts as a pigmented diffuse reflector) onto the rear surface of poly-Si thin-film solar cells on glass ("ALICIA cells") strongly improves the  $J_{sc}$ , whereas deposition of an Al film degrades

TABLE 1: Results of 1-Sun  $I$ - $V$  measurements on 4 different PLASMA cells, also shown (column  $J_{sc,EQE}$ ) is the 1-Sun  $J_{sc}$  under AM1.5G illumination calculated from the measured EQE curve.

Sample	Glass surface	Si thickness (nm)	$V_{oc}$ (mV)	$J_{sc}$ (mA/cm <sup>2</sup> )	$FF$ (%)	Eff (%)	$J_{sc,EQE}$ (mA/cm <sup>2</sup> )
3.3 $\mu$ m-P	Planar	$\sim 3300$	442	13.8	68.0	4.2	14.71
3.3 $\mu$ m- $\text{Tex}$	Textured (AIT-175 nm)	$\sim 3300$	461	16.0	67.4	5.0	17.25
5.0 $\mu$ m-PI	Planar	$\sim 5000$	448	17.4	63.6	5.1	18.92
5.0 $\mu$ m- $\text{Tex}$	Textured (AIT-175 nm)	$\sim 5000$	445	19.6	63.2	5.5	19.98

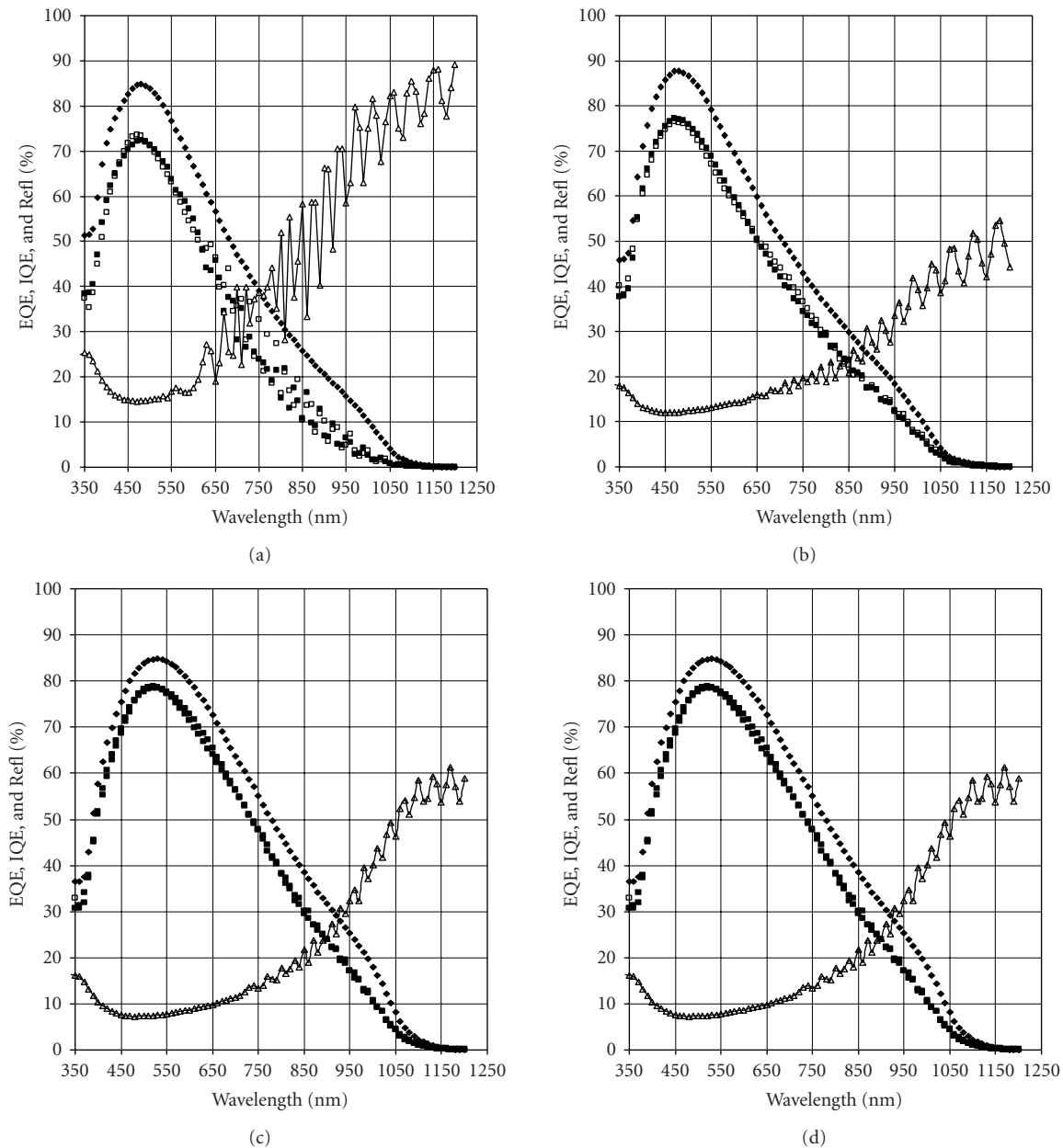


FIGURE 7: Measured EQE (open squares) and reflectance (open triangles) of PLASMA solar cells, also shown are the PC1D-simulated EQE and IQE curves (filled squares and filled diamonds). Graph (a) = sample 3.3  $\mu$ m-PI, graph (b) = sample 3.3  $\mu$ m- $\text{Tex}$ , graph (c) = sample 5.0  $\mu$ m-PI, graph (d) = sample 5.0  $\mu$ m- $\text{Tex}$ .

TABLE 2: PC1D simulation parameters of planar and AIT-textured PLASMA poly-Si solar cells, as obtained from fitting of the cells' measured EQE curves.

Sample	3.3 $\mu\text{m}$ -Pl	3.3 $\mu\text{m}$ -Tex	5.0 $\mu\text{m}$ -Pl	5.0 $\mu\text{m}$ -Tex
Thickness of emitter (nm)	70	80	70	100
Doping level in emitter ( $\text{cm}^{-3}$ )	$4 \times 10^{19}$	$6 \times 10^{19}$	$6 \times 10^{19}$	$6 \times 10^{19}$
Diffusion length in emitter (nm)	75	75	65	90
Thickness of $n$ -type part of absorber (nm)	750	800	1000	1000
Doping level in $n$ -type part of absorber ( $\text{cm}^{-3}$ )	$1 \times 10^{16}$	$1 \times 10^{16}$	$1 \times 10^{16}$	$1 \times 10^{16}$
Diffusion length in $n$ -type part of absorber (nm)	1300	1200	1300	1150
Thickness of $p$ -type part of absorber (nm)	2050	2200	4000	4000
Doping level in $p$ -type part of absorber ( $\text{cm}^{-3}$ )	$1 \times 10^{16}$	$1 \times 10^{16}$	$1 \times 10^{16}$	$1 \times 10^{16}$
Diffusion length in $p$ -type part of absorber (nm)	2050	2500	5000	5600
Internal reflection front surface (%)	52	94	50	94
Internal reflection rear surface (%)	48	25	52	28

the  $J_{sc}$  (whereby the degradation was found to be particularly strong for textured samples). The important result from these investigations is that evaporated Al on poly-Si films is a poor back surface reflector, and particularly so for textured samples. Work is under way in our group to replace the full-area aluminium BSR by localised Al contacts and to cover the nonmetallised rear surface regions with a good BSR such as white paint.

### 3.3. 7% efficient PLASMA cells

By further optimising the solar cell fabrication process (RTA, hydrogenation, etc.), we have been able to improve the 1-Sun  $V_{oc}$  of AIT-textured PLASMA samples to up to 491 mV and the  $FF$  to over 70%. In Figure 8, the measured 1-Sun current-voltage and power-voltage curves of the best PLASMA cell fabricated as yet by us is shown. The cell has an energy conversion efficiency (total area) of 7.0%, a  $V_{oc}$  of 491 mV, a  $FF$  of 70.5%, and a  $J_{sc}$  of 20.1 mA/cm<sup>2</sup>. Total cell area is 4.40 cm<sup>2</sup> and the silicon thickness is 4.0  $\mu\text{m}$ . The  $I$ - $V$  curve was measured using an aperture mask with an area of 4.40 cm<sup>2</sup>. From the measured EQE curve of this AIT-textured cell, a  $J_{sc,EQE}$  of 20.55 mA/cm<sup>2</sup> is obtained for the AM1.5G spectrum. It is noted that this 7% PLASMA cell has a full-area Al rear contact and hence relatively modest light trapping properties. Significant improvements of the short-circuit current (and hence the cell efficiency) are expected from the implementation of an improved back surface reflector, as discussed in the previous section.

## 4. CONCLUSIONS

A new glass texturing method (AIT—aluminium-induced texturing) has recently been developed by our group. In the present work, the potential of this method has been explored by fabricating PLASMA poly-Si thin-film solar cells on glass superstrates that were textured with the AIT method. Using an interdigitated metallisation scheme with a full-area Al rear contact, PLASMA cells with an efficiency of up to 7.0% have been realised. This promising result shows that the AIT glass texturing method is fully compatible with the fab-

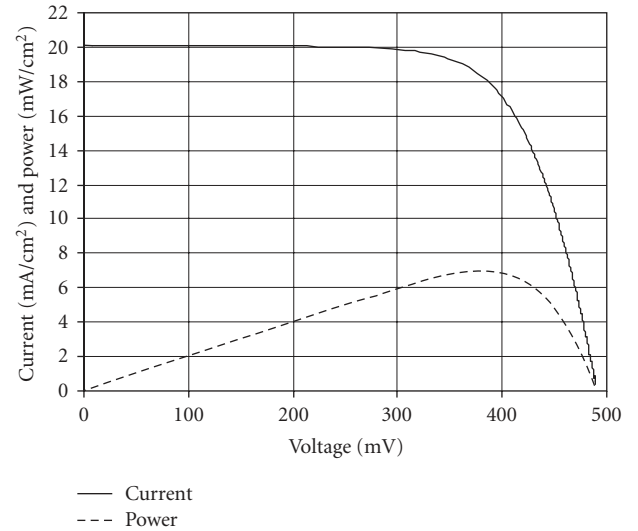


FIGURE 8: Measured current-voltage and power-voltage curves of a 7.0% efficient PLASMA solar cell made on AIT-textured glass (silicon thickness 4  $\mu\text{m}$ , total cell area 4.40 cm<sup>2</sup>, approximated AM1.5G spectrum, 100 mW/cm<sup>2</sup>, cell temperature 25°C).

rication of poly-Si thin-film solar cells on glass using solid phase crystallisation (SPC) of PECVD-deposited amorphous silicon precursor diodes. As such, there are now two distinctly different glass texturing methods—the AIT method and CSG solar's glass bead method [13]—that are known to be capable of producing efficient SPC poly-Si thin-film solar cells on glass.

While short-circuit current densities  $J_{sc}$  of up to 20 mA/cm<sup>2</sup> have been realised in the present paper, the  $J_{sc}$  potential of the AIT glass texturing method is actually significantly higher, as confirmed by optical absorption measurements taken on the samples prior to metallisation (i.e., using air as the back surface reflector). The reason why the present textured cells have relatively modest  $J_{sc}$  has been shown to be the poor internal reflectance of about 25% at the textured, full-area rear Al contact. By implementing a locally

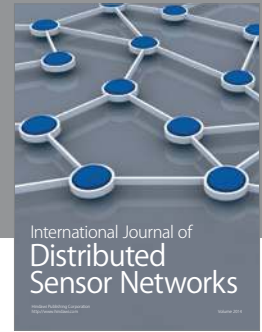
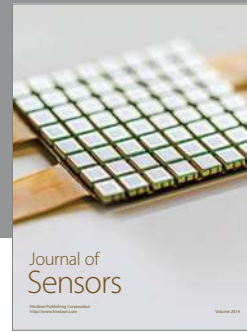
contacting rear Al electrode and a pigmented diffuse reflector (such as white paint [12]) in the metal-free rear surface regions, the  $J_{sc}$  can be significantly boosted.

## ACKNOWLEDGMENTS

This work has been supported by the Australian Research Council (ARC) via its Centres of Excellence scheme. The authors acknowledge the contributions of present and former members of the Thin-Film Group at UNSW.

## REFERENCES

- [1] T. Matsuyama, N. Terada, T. Baba, et al., "High-quality polycrystalline silicon thin film prepared by a solid phase crystallization method," *Journal of Non-Crystalline Solids*, vol. 198–200, part 2, pp. 940–944, 1996.
- [2] M. A. Green, P. A. Basore, N. Chang, et al., "Crystalline silicon on glass (CSG) thin-film solar cell modules," *Solar Energy*, vol. 77, no. 6, pp. 857–863, 2004.
- [3] P. A. Basore, "CSG-2: expanding the production of a new polycrystalline silicon PV technology," in *Proceedings of the 21st European Photovoltaic Solar Energy Conference*, pp. 544–548, Dresden, Germany, September 2006.
- [4] N. Chuangsuwanich, P. I. Widenborg, P. Campbell, and A. G. Aberle, "Light trapping properties of thin silicon films on AIT-textured glass," in *Proceedings of the 14th International Photovoltaic Science and Engineering Conference (PVSEC'04)*, pp. 325–326, Bangkok, Thailand, January 2004.
- [5] A. G. Aberle, P. I. Widenborg, and N. Chuangsuwanich, "Glass texturing," International PCT patent application WO 2004/089841 A1, 2004.
- [6] A. G. Aberle, "Recent progress in poly-Si thin-film solar cells on glass," in *Proceedings of the 21st European Photovoltaic Solar Energy Conference*, pp. 738–741, Dresden, Germany, September 2006.
- [7] M. L. Terry, A. Straub, D. Inns, D. Song, and A. G. Aberle, "Large open-circuit voltage improvement by rapid thermal annealing of evaporated solid-phase-crystallized thin-film silicon solar cells on glass," *Applied Physics Letters*, vol. 86, no. 17, Article ID 172108, 3 pages, 2005.
- [8] T. M. Walsh, D. Song, S. Motahar, and A. G. Aberle, "Self-aligning maskless photolithography method for metallising thin-film crystalline silicon solar cells on transparent supporting materials," in *Proceedings of the 15th International Photovoltaic Science and Engineering Conference (PVSEC '05)*, p. 706, Shanghai, China, October 2005.
- [9] P. A. Basore, "Numerical modeling of textured silicon solar cells using PC-1D," *IEEE Transaction on Electron Devices*, vol. 37, no. 2, pp. 337–343, 1990.
- [10] P. Campbell, P. I. Widenborg, A. B. Sproul, and A. G. Aberle, "Surface textures for large-grained poly-silicon thin-film solar cells on glass using the AIT method," in *Proceedings of the 15th International Photovoltaic Science and Engineering Conference (PVSEC '05)*, pp. 859–860, Shanghai, China, October 2005.
- [11] P. I. Widenborg and A. G. Aberle, "Hydrogen-induced dopant neutralisation in p-type AIC poly-Si seed layers functioning as buried emitters in ALICE thin-film solar cells on glass," *Journal of Crystal Growth*, vol. 306, no. 1, pp. 177–186, 2007.
- [12] O. Berger, D. Inns, and A. G. Aberle, "Commercial white paint as back surface reflector for thin-film solar cells," *Solar Energy Materials and Solar Cells*, vol. 91, no. 13, pp. 1215–1221, 2007.
- [13] J. J. Ji and Z. Shi, "Texturing of glass by SiO<sub>2</sub> film," US patent 6,420,647, 2002.



**Hindawi**

Submit your manuscripts at  
<http://www.hindawi.com>

